# Dynamics of $He^{2+}+H(1s)$ ionization with screened Coulomb interactions

L. Liu,[1] J. G. Wang,[1] and R. K. Janev[2]
[1]*The Key Laboratory of Computational Mathematics, Institute of Applied Physics and Computational Mathematics, P.O. Box 8009, Beijing 100088, People's Republic of China*
[2]*Macedonian Academy of Sciences and Arts, P.O. Box 428, 1000 Skopje, Macedonia*
(Received 22 February 2008; published 15 April 2008)

Collision dynamics of $He^{2+}+H(1s)$ ionization in a hot, dense (Debye) plasma is studied by the two-center atomic orbital close-coupling (AOCC) method in the energy range 5–300 keV/u. The target AO basis contained all $n\leq 6$ bound states and 117 quasicontinuum states, while that on the projectile contained all $n\leq 4$ bound states. The eigenenergies and wave functions of all these states were obtained variationally as a function of the screening parameter in a Debye-Hückel potential and used in AOCC dynamics calculations. With increasing the screening, more and more discrete states enter the target and projectile continuum and increase the ionization cross section, particularly at low collision energies. The ionization to target continuum is the main ionization channel, while the ionization to the projectile continuum becomes important only for large screenings and collision energies below ~50 keV/u.

DOI: 10.1103/PhysRevA.77.042712 PACS number(s): 34.20.Cf, 34.50.Fa, 52.30.−q

## I. INTRODUCTION

Atomic collision processes in hot, dense plasmas play a crucial role in determining their radiation and transport properties and therefore have been subject to continuous interest during the last several decades [[1–5], and references herein]. Theoretical studies of these processes have covered both electron-impact excitation [2,6–9] and ionization [10] of hydrogenlike ions, as well as the proton-impact excitation of $n=2$ fine structure levels of hydrogenlike ions [11], electron capture in proton/fully stripped ion-hydrogenlike ion collisions [12,13], and a classical trajectory Monte Carlo (CTMC) study of electron capture and ionization in hydrogen atom-fully stripped ion collisions [14]. In most of these studies the plasma screening of Coulomb interactions has been represented by a Debye-Hückel potential (weakly coupled plasmas) and the collision dynamics described within the perturbation theory framework. Only in Ref. [11] a two-state close coupling description of collision dynamics was used for both weakly and strongly coupled plasmas. In the latter case the screening has been described by the ion-sphere model potential [1]. The ion-sphere model potential has been also used in the symmetric charge transfer cross section calculations of Ref. [13]. We would like to note that in all these studies, except for Ref. [14], the change of energies and wave functions of atomic bound states in the screened Coulomb potential were taken into account at most only within the first order perturbation theory. In the CTMC calculations of electron capture and ionization processes in $H(1s)$-fully stripped ion collisions of Ref. [14], the microcanonical distribution of the initial bound $H(1s)$ state and the energies of capture states on the projectile (in the sense of quantum-classical correspondence) were determined by using the Debye-Hückel potential.

In the present work we shall study the ionization process in $He^{2+}+H(1s)$ collisions,

$$He^{2+} + H(1s) \rightarrow He^{2+} + H^{+} + e, \tag{1}$$

when the interaction of the electron with an ion with positive charge $Z$ at a distance $r$ is given by the screened Coulomb potential of Debye-Hückel form ($e$ is the unit charge)

$$V(r) = -\frac{Ze^2}{r} e^{-r/\lambda_D}. \tag{2}$$

In the case when the collision takes place in a weakly coupled (Debye) plasma the screening length is given by $\lambda_D=(k_BT_e/4\pi e^2 n_e)^{1/2}$, where $T_e$ and $n_e$ are the plasma electron temperature and density, respectively, and $k_B$ is the Boltzmann constant. The representation of charged particle interaction in a plasma by the potential (2) is adequate only if the Coulomb coupling parameter $\Gamma=e^2/(ak_BT_e)$ and plasma nonideality parameter $\gamma=e^2/(\lambda_D k_B T_e)$ satisfy the conditions $\Gamma \leq 1$, $\gamma \ll 1$, where $a=[3/(4\pi n_e)]^{1/3}$ is the average interparticle distance.

We shall study the dynamics of the process (1) by employing the two-center atomic orbital close-coupling (TCAOCC) method [15] with plane wave electron translational factors (PWETFs) in the energy range 5–300 keV/u. The atomic orbitals, including those representing the continuum, are determined variationally from the corresponding single-center Schrödinger equation with the potential (2) and the couplings are calculated with the interaction (2) between any two charged particles in the system. The main objective of the present study is to investigate how the screened Coulomb interaction (2) affects the dynamics of the ionization process when the screening length $\lambda_D$ varies.

We note that the dynamics of excitation and electron capture processes in the $He^{2+}+H(1s)$ collision system with screened Coulomb interactions (2) between the particles has been investigated recently [16] with the same approach used here. The results of that study have shown that the screening of Coulomb interactions in the collision system has dramatic effects on the dynamics of excitation and electron capture processes, leading in particular to reduction of the open inelastic channels with increasing the screening and to significant changes in the magnitude and energy behavior of the cross sections of open channels. We further note that in the unscreened case, the ionization process (1) has been subject

 

to numerous theoretical studies employing various methods, the most extensive of which in the intermediate to high energy region are the TCAOCC calculations of Refs. [17,18] employing large AO basis sets.

The paper is organized as follows. In the next section we briefly outline the theoretical method used in the cross-section calculations, with emphasis on the specific features that the screened Coulomb interaction (2) introduces in the AO basis and dynamical couplings. In Sec. III we present and analyze our cross-section results for the process (1) when the screening length $\lambda_D$ varies. In Sec. IV we give our conclusions. Atomic units will be used in the remaining part of this paper unless explicitly indicated otherwise.

## II. THEORETICAL METHOD

### A. Atomic orbitals and energies of the screened Coulomb potential

The application of the TCAOCC method to an ion-atom collision system requires determination of single-center electronic states, including those lying in the continuum (pseudostates) over which the total scattering wave function is expanded and used in the time-dependent Schrödinger equation to generate the coupled equations for the state amplitudes [15]. For description of the ionization process it is essential that the number of target-centered quasicontinuum states should be sufficiently large to ensure adequate representation of the continuum and achieve convergence of the results [17,18]. For determining the stationary bound and quasicontinuum states with the potential (2) centered on the target ($Z=1$) and on the projectile ($Z=2$), we have used the variational method with even-tempered trial functions [18,19]

$$\chi_{klm}(\vec{r};\lambda_D) = N_l[\xi_k(\lambda_D)]r^l e^{-\xi_k(\lambda_D)r} Y_{lm}(\hat{\vec{r}}),$$

$$\xi_k(\lambda_D) = \alpha\beta^k, \quad k = 1,2,\ldots,N, \tag{3}$$

where $N_l(\xi_k)$ is a normalization constant, $Y_{lm}(\hat{\vec{r}})$ are the spherical harmonics, and $\alpha$ and $\beta$ are variational parameters, determined by minimization of the energy for each value of $\lambda_D$. The atomic states $\phi_{nlm}(\vec{r};\lambda_D)$ are then obtained as the linear combination

$$\phi_{nlm}(\vec{r};\lambda_D) = \sum_k c_{nk}\chi_{klm}(\vec{r};\lambda_D), \tag{4}$$

where the coefficients $c_{nk}$ are determined by diagonalization of a single-center Hamiltonian. This diagonalization yields the energies $E_{nl}(\lambda_D)$ of the atomic states in the screened Coulomb potential (2).

A specific feature of the screened Coulomb potential (2) is that it supports only a finite number of bound, nondegenerate states [20] for any finite value of $\lambda_D$. This implies that with decreasing the Debye length $\lambda_D$, each of the bound states from the single-center basis will enter the continuum at a certain value of screening length $\lambda_{D,c}^{n,l}$ and become a quasicontinuum state. The reduction of bound atomic states and the increase of the quasicontinuum states with decreasing $\lambda_D$ have an obvious effect on the collision dynamics.

In the present calculations we have included in the basis all the $n \leq 6$ and $7s$ discrete states and 117 quasicontinuum states centered on the target (in total 174 states) and all the states with $n \leq 4$ centered on the projectile, with no projectile-centered pseudostates (at $\lambda_D = \infty$). This basis was necessary and sufficient to reach converged results for the ionization cross section in the unscreened case. We note that in the ionization calculations of Ref. [18] the same number of target basis functions was used, but the basis centered on the projectile included all the states with $n \leq 5$ (and no quasicontinuum states). In Ref. [17] the target basis functions included all $n \leq 4$ discrete and 84 quasicontinuum states, while those centered on the projectile included all the states with $n \leq 5$ and 61 quasicontinuum states. In selecting to exclude the projectile-centered quasicontinuum states in the basis we were guided by the arguments given in Refs. [18,21], demonstrating that the use of projectile-centered quasicontinuum states does not improve the excitation or ionization cross-section results, provided the target-centered discrete and quasicontinuum basis is sufficiently large. As we shall see later (Sec. III) our total ionization cross section for the unscreened case practically coincides with that of Ref. [18] in the energy region above 20 keV/u (where the two sets of data overlap) and is slightly below (less than 8%) the result of Ref. [17] in the energy range 40–80 keV/u. An additional reason for excluding the projectile-centered quasicontinuum states from our basis was the fact that the main purpose of the present study is not to achieve a highly accurate ionization cross-section result for the unscreened case, but rather to study the ionization dynamics when the screening parameter in the Coulomb interaction varies. In view of the emergence of new quasicontinuum states centered on the projectile when the Debye length decreases (that originate from the discrete $He^+$ capture states), one can observe in a transparent way the contribution to the total ionization from these projectile-centered pseudostates.

In Fig. 1 we show the $\lambda_D$ dependence of the energies $E_{nl}$ of $n \leq 3$ bound states [panel (a)] and of several quasicontinuum states [panel (b)] of the target-centered basis. The dashed lines in Fig. 1(a) represent the results of numerical solution of the Schrödinger equation [22]. It should be noted in Fig. 1(a) that the considered $n \leq 3$ energy levels rapidly approach the continuum edge for $\lambda_D$ below $20-30a_0$ and enter the continuum at a certain critical value $\lambda_{D,c}^{n,l}$ of the screening length. The energies of quasicontinuum states [Fig. 1(b)] also increase with decreasing $\lambda_D$, this increase being more rapid for the states with higher angular momentum (just as in the case of discrete states). In Fig. 1(b) we also show the $\lambda_D$ dependence of energies of the $6s$ and $7s$ states that at zero screening are discrete (with energies of −0.013 82 and −0.009 71 a.u., respectively) but become quasicontinuum states for $\lambda_D$ smaller than $\approx 32a_0$ and $\approx 53a_0$, respectively. The continuity of the energy of these states when passing the critical Debye length reflects the fact that they preserve their character (square integrability) in both the discrete and continuum spectrum.

In Tables I and II we give the values of critical Debye lengths, $\lambda_{D,c}^{n,l}$, for the $n \leq 5$ states of H and $He^+$. The values for the H states are compared with those from the numerical

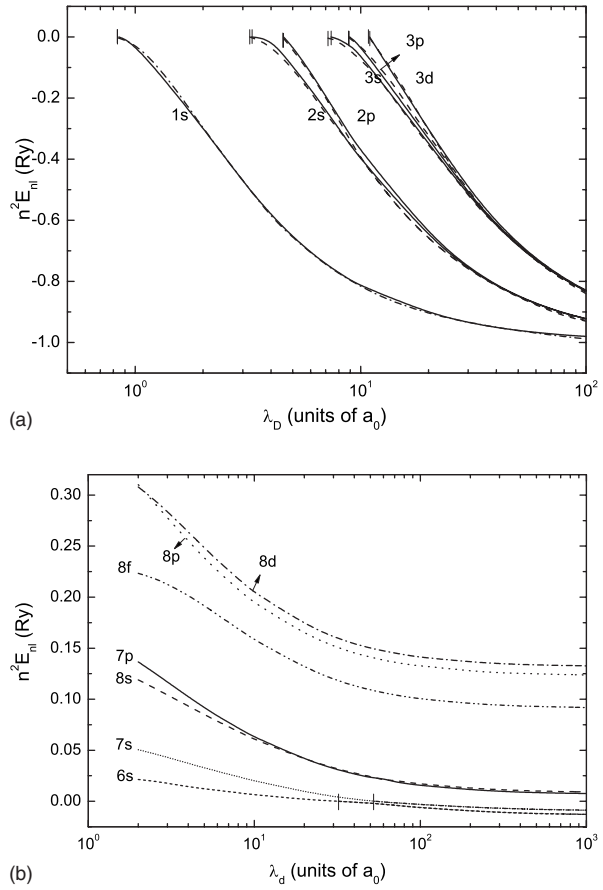


FIG. 1. Dependence of binding energies on $\lambda_D$ of the $n \leq 3$ discrete states (a) and of a number of quasicontinuum states (b) centered on H. The dashed lines in (a) are the results of Ref. [22].

solution of the Schrödinger equation [22] (given in parentheses), indicating the good accuracy of the present variational calculations.

### B. TCAOCC coupled equations

Within the semiclassical approximation, the electron wave function of the $He^{2+}+H(1s)$ collision system $\Psi(\vec{r},t;\lambda_D)$ satisfies the equation

TABLE I. Critical screening lengths, $\lambda_{D,c}^{n,l}$ $(a_0)$, for H $(nl)$ states, $n \leq 5$.

| $n\backslash l$ | 0 | 1 | 2 | 3 | 4 |
|---|---|---|---|---|---|
| 1 | 0.8450 | | | | |
| | (0.8399)[a] | | | | |
| 2 | 3.280 | 4.542 | | | |
| | (3.223) | (4.541) | | | |
| 3 | 7.380 | 8.900 | 10.950 | | |
| | (7.171) | (8.872) | (10.947) | | |
| 4 | 12.750 | 14.980 | 17.250 | 20.080 | |
| | (12.687) | (14.731) | (17.210) | (20.068) | |
| 5 | 21.260 | 23.550 | 25.400 | 28.550 | 34.600 |
| | (19.772) | (22.130) | (24.985) | (28.257) | (31.904) |

[a]The values in parentheses are from Ref. [22].

TABLE II. Critical screening lengths, $\lambda_{D,c}^{n,l}$ $(a_0)$, for $He^+(nl)$ states, $n \leq 5$.

| $n\backslash l$ | 0 | 1 | 2 | 3 | 4 |
|---|---|---|---|---|---|
| 1 | 0.42715 | | | | |
| 2 | 1.67800 | 2.2725 | | | |
| 3 | 3.87300 | 4.4920 | 5.4817 | | |
| 4 | 7.39500 | 7.8690 | 8.8520 | 10.120 | |
| 5 | 14.2800 | 14.045 | 15.015 | 16.020 | 17.415 |

$$\left(H - i\frac{\partial}{\partial t}\right)\Psi(\vec{r},t;\lambda_D) = 0, \tag{5}$$

where

$$H = -\frac{1}{2}\nabla_r^2 + V_A(r_A;\lambda_D) + V_B(r_B;\lambda_D) \tag{6}$$

and $V_{A,B}(r_{A,B};\lambda_D)$ are the electron interactions with the target proton (subscript A) and projectile ion $He^{2+}$ (subscript B) of the form (2). In the collision energy range considered in the present paper (5–300 keV/u), the straight-line approximation for the relative nuclear motion, $R(t)=\vec{b}+\vec{v}t$ ($b$ is the impact parameter and $v$ is the collision velocity), can be safely adopted [15], particularly having in mind that the nucleus-nucleus interaction is also screened. Expanding the wave function $\Psi(\vec{r},t)$ in terms of atomic orbitals (4), multiplied by plane wave translational factors [15] [to generate "traveling" atomic orbitals, $\phi^{A,B}(\vec{r},t;\lambda_D)$]

$$\Psi(\vec{r},t) = \sum_i a_i(t)\phi_i^A(\vec{r},t;\lambda_D) + \sum_j b_j(t)\phi_j^B(\vec{r},t;\lambda_D), \tag{7}$$

and inserting it into Eq. (5), one obtains the system of coupled equations for the amplitudes $a_i(t)$ and $b_j(t)$ [15]

$$i(\dot{A} + S\dot{B}) = HA + KB, \tag{8a}$$

$$i(\dot{B} + S^\dagger\dot{A}) = \bar{K}A + \bar{H}B, \tag{8b}$$

where $A$ and $B$ are the vectors of amplitudes $a_i$ and $b_j$, respectively, $S$ is the overlap matrix ($S^\dagger$ is its transposed form), $H$ and $\bar{H}$ are direct coupling matrices on the target and projectile, and $K$ and $\bar{K}$ are the electron exchange matrices. We note that the functions $\phi^{A,B}(\vec{r},t;\lambda_D)$ in the expansion (7) include both the discrete and quasicontinuum states on the respective center. The system of equations (8) is to be solved under the initial conditions

$$a_i(-\infty) = \delta_{1i}, \quad b_j(-\infty) = 0. \tag{9}$$

After solving the system of coupled equations (8), the ionization cross section (at a given value of $\lambda_D$) is calculated as the sum

$$\sigma_{ion} = \sigma_{ion}^{tc} + \sigma_{ion}^{pc}, \tag{10}$$

$$\sigma_{ion}^{tc} = 2\pi\sum_i \int_0^\infty |a_i^c(+\infty)|^2 b db, \tag{11a}$$

$$\sigma_{ion}^{pc} = 2\pi \sum_j \int_0^\infty |b_j^c(+\infty)|^2 b db, \tag{11b}$$

where $a_i^c$ and $b_j^c$ are the amplitudes of the quasicontinuum states centered on the target and projectile, respectively, and the summations in Eqs. (11) run over the corresponding quasicontinuum states available at a given value of $\lambda_D$. We should note that, in accordance with the adopted basis in the present calculations, the term $\sigma_{ion}^{pc}$ will be different from zero only for $\lambda_D \leq 10.12a_0$, the critical Debye length at which the $4f$ discrete state of $He^+$ enters the continuum (see Table II).

### C. Couplings

Within the TCAOCC approach to ion-atom collision dynamics the continuum is represented by the quasicontinuum states included in the basis. Transitions to these quasicontinuum states from the initial target state can take place either directly or via intermediate discrete states on each of the centers. As we have mentioned earlier, in the case of screened Coulomb potential the number of quasicontinuum states around each of the centers increases with decreasing the screening length since for $\lambda_D \leq \lambda_{Dc}^{nl}$ each discrete $n,l$-state becomes a quasicontinuum state (see Fig. 1). On this basis, one would expect that the ionization cross section should increase with decreasing the screening length. As we shall see in the next section, this is indeed so down to certain values of $\lambda_D$. However, since the number of intermediary discrete states also decreases with decreasing $\lambda_D$ (reducing, thus, the strong intermediate transition steps promoting the probability flux toward the continuum), the ionization cross section may start to decrease for the very small values of $\lambda_D$.

In order to gain an insight into the ionization dynamics, we shall present the behavior of some of the matrix elements $H_{i,i'}$ and $K_{i,j'}$, the former coupling the states centered on the target and the latter coupling the target states with those on the projectile; and in which the final state is a quasicontinuum state.

In Figs. 2(a)–2(c) we present the dependence on internuclear distance R of matrix elements for the direct transitions from H($1s$) to target quasicontinuum states $8s$, $7p$, and $8p$, respectively, for screening lengths $\lambda_D = 12, 8, 6, 4$, and $2a_0$. The values of the matrix element for the $1s$-$8s$ transition [Fig. 2(a)] maximize at small internuclear distances and rapidly increase below $R \sim 4a_0$ with decreasing $\lambda_D$ down to $\lambda_D = 4a_0$. For $\lambda_D = 2a_0$, however, the $1s$-$8s$ coupling is weaker than for $\lambda_D = 4a_0$. The matrix elements for $1s$-$7p$ and $1s$-$8p$ transitions [Figs. 2(b) and 2(c)] are both peaked at $R \approx 1.5a_0$. In the R region around the peaks, the values of $1s$-$7p$ coupling first increase with the decrease of $\lambda_D$ (up to $\lambda_D = 6a_0$) and then start to decrease, while those for the $1s$-$8p$ coupling show a slight decrease with decreasing $\lambda_D$, except for the strong decrease for $\lambda_D = 2a_0$. The decrease of direct coupling elements for $\lambda_D \leq 4a_0$ was observed also for $1s$-$8d$ and all other transitions to higher $l$. The observed $\lambda_D$ behavior of the direct coupling matrix elements $H_{ij'}$ indicates that their contribution to the population of target continuum states (ionization to target continuum) first increases with decreasing $\lambda_D$, and then (for $\lambda_D \leq 4a_0$) decreases. We should note, however, that the target continuum states can be indirectly populated also by transitions from the intermediate $He^+$-capture states. The contribution from such two-step transitions to the target ionization continuum is, however, small, except for those from the intermediate $2s(He^+)$ and

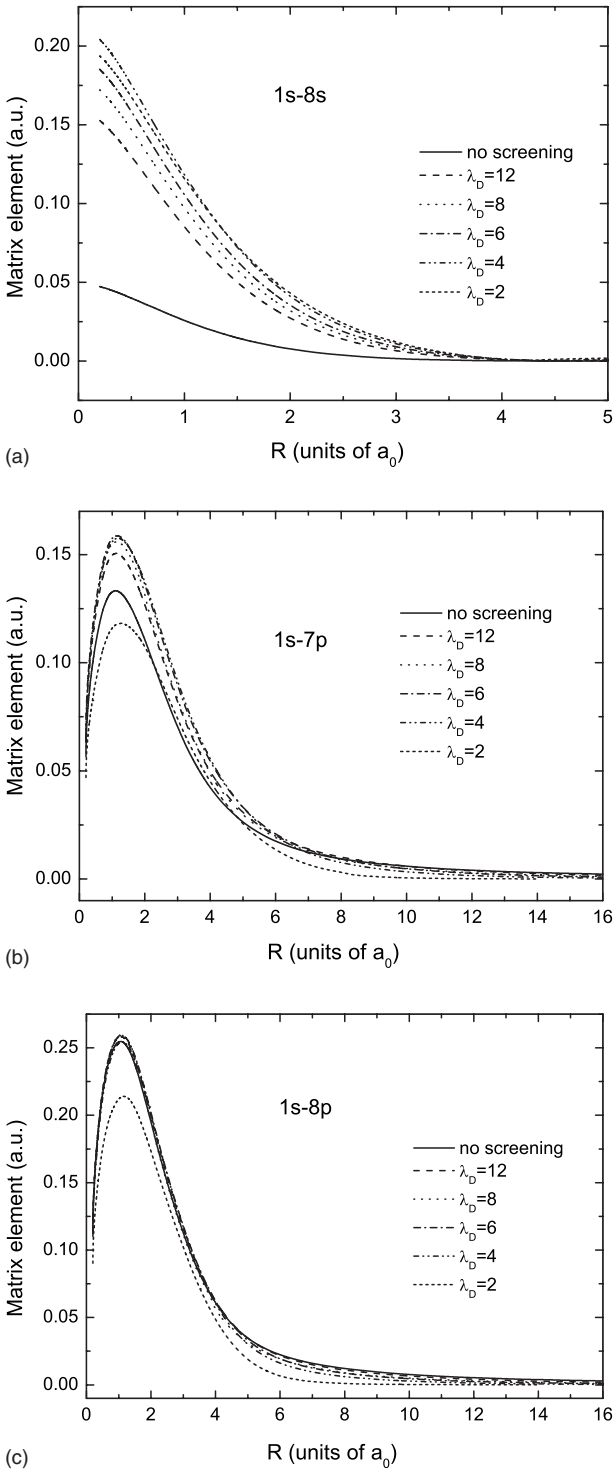


FIG. 2. Radial variation of matrix elements for direct transitions from H($1s$) to target quasicontinuum states $8s$ (a), $7p$ (b), and $8p$ (c) for zero screening and for interaction screening with $\lambda_D = 12, 8, 6, 4$, and $2a_0$.

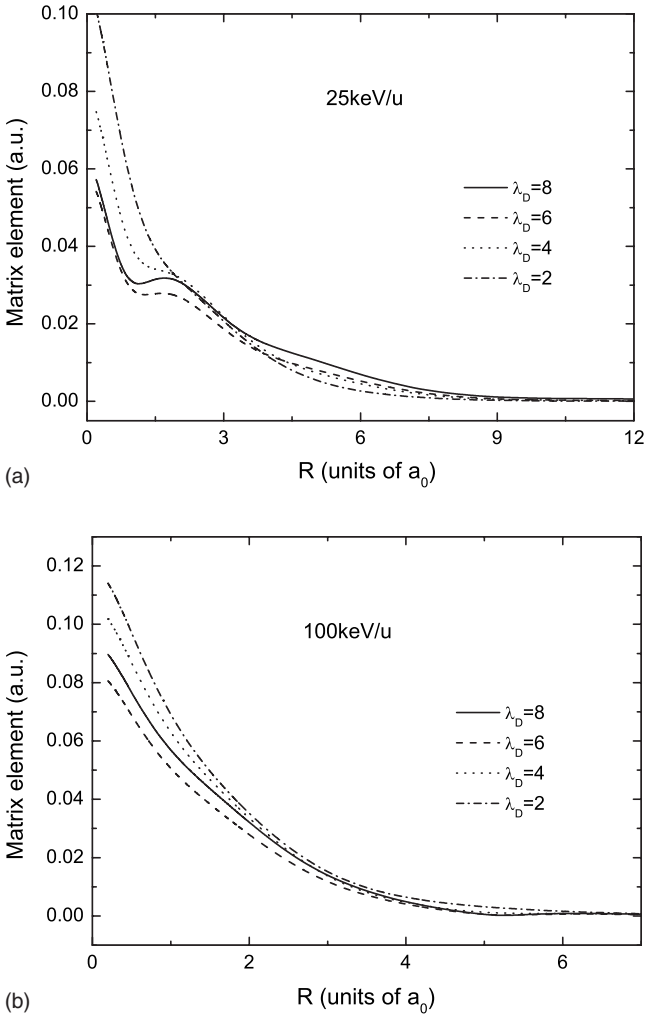


FIG. 3. Absolute values of exchange matrix elements for the transition $1s$(H)-$4s$($He^+$) at collision energies of 25 keV/u (a) and 100 keV/u (b) for the screened cases with $\lambda_D=8,6,4$, and $2a_0$.

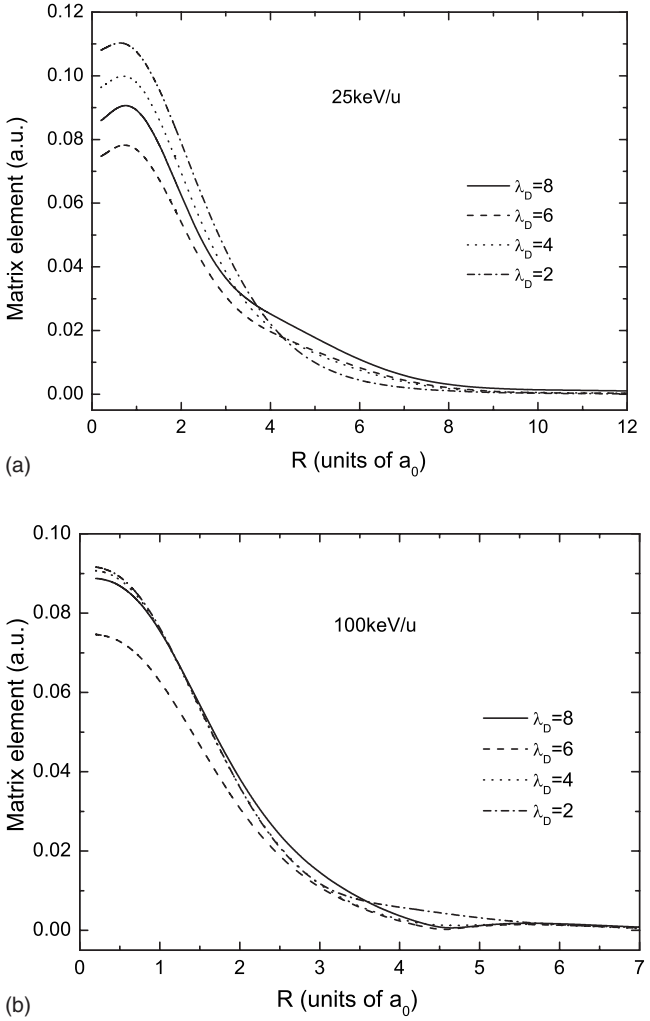


FIG. 4. Same as in Fig. 3, but for the transition $1s$(H)-$4p$($He^+$).

$2p$($He^+$) capture states that are energetically resonant with the initial $1s$(H) state (and thereby strongly coupled with it).

Figures 3 and 4 show the absolute values of exchange matrix elements for the transitions $1s$(H)-$4s$($He^+$) (Fig. 3) and $1s$(H)-$4p$($He^+$) (Fig. 4) transitions at collision energies of 25 keV/u [panels (a)] and 100 keV/u [panels (b)] for the screened cases with $\lambda_D=8,6,4$, and $2a_0$. We note that for the screened case $\lambda_D=8a_0$, the $4s$($He^+$) and $4p$($He^+$) states are still in the discrete spectrum, while for the other screening lengths they lie in the continuum (see Table II). A general feature of the exchange matrix elements shown in these figures is that with respect to the $\lambda_D=8a_0$ case their magnitude in the low R region (where they attain their maximum values) first decreases with decreasing of $\lambda_D$ (e.g., for $\lambda_D=6a_0$) and then it increases (for $\lambda_D \leq 4a_0$). This indicates that the population of projectile continuum states (i.e., capture to the projectile continuum) becomes significant in the screening region with $\lambda_D \leq 4a_0$ in which the direct coupling with the target continuum states decreases with decreasing $\lambda_D$ (see Fig. 2 and related discussions).

## III. CROSS SECTIONS

### A. Probabilities for population of specific quasicontinuum states

An insight into the ionization dynamics in collisions with screened Coulomb interactions of Debye-Hückel (Yukawa) type can be gained also by considering the ionization probabilities to specific quasicontinuum states as a function of impact parameter, $P(b)$. We show the weighted probabilities $bP(b)$ as a function of impact parameter $b$ for population of the $7s$, $7p$, and $8p$ target quasicontinuum states for the unscreened case and for interaction screening with $\lambda_D=12,6,4,2.5$, and $2a_0$ at collision energies of 25 and 100 keV/u, respectively. We note that for the zero screening the $7s$ state is bound, but for $\lambda_D \leq 52a_0$ it becomes a quasicontinuum state [see Fig. 1(b)]. [This explains the displacement of the maximum of $bP(b)$ for this state in the zero screening case in panels (a) of Figs. 5 and 6 with respect to the maxima for the finite values of $\lambda_D$.] Figures 5(a)–5(c) show that the weighted population probability of a quasicontinuum state increases with decreasing $\lambda_D$ at this collision energy. Another specific feature of $bP(b)$curves for E

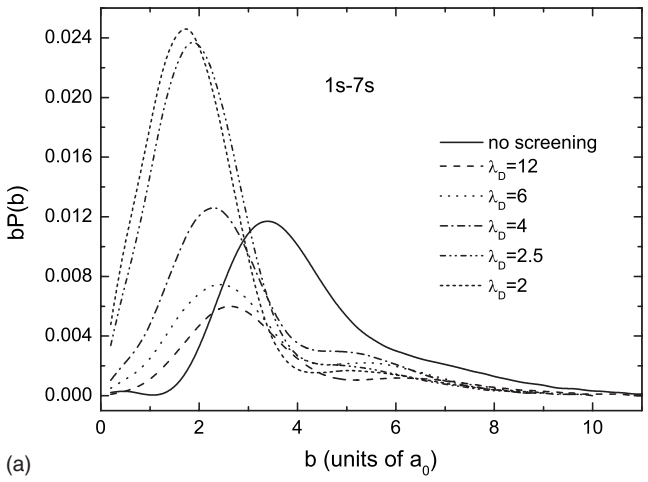


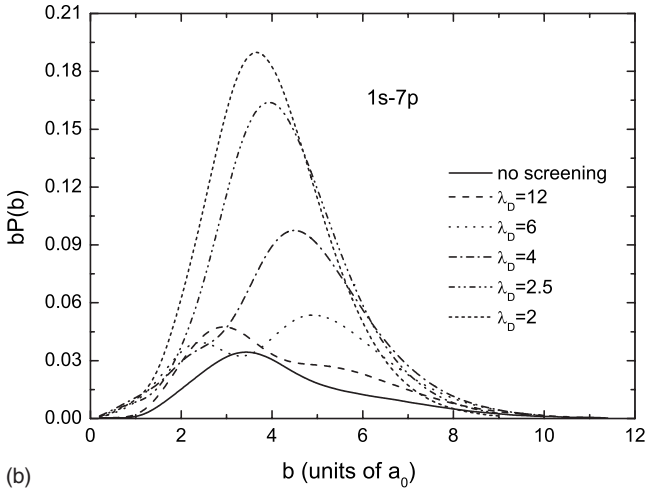


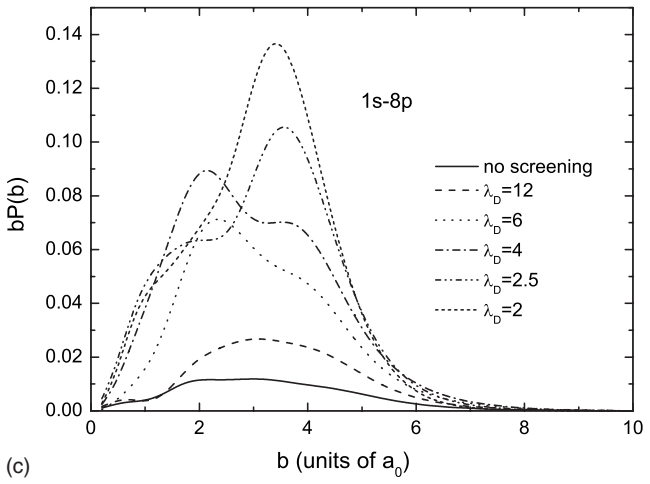


FIG. 5. Weighted probabilities $bP(b)$ as a function of impact parameter for the population of $7s$ (a), $7p$ (b), and $8p$ (c) target quasicontinuum states for zero screening and for screening with $\lambda_D=12,6,4,2.5$, and $2a_0$ at the collision energy of 25 keV/u.

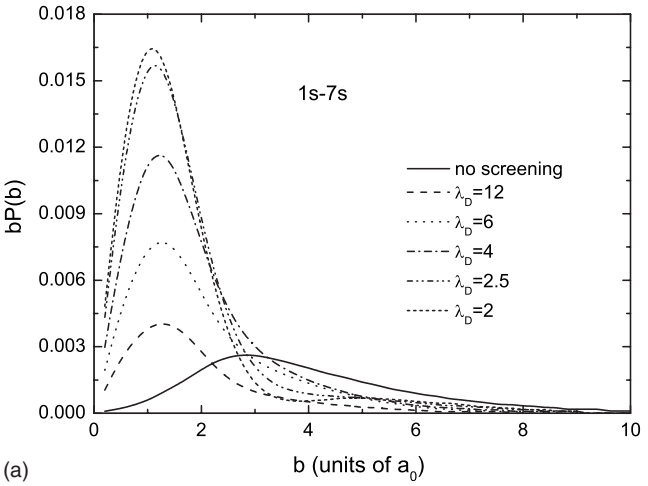


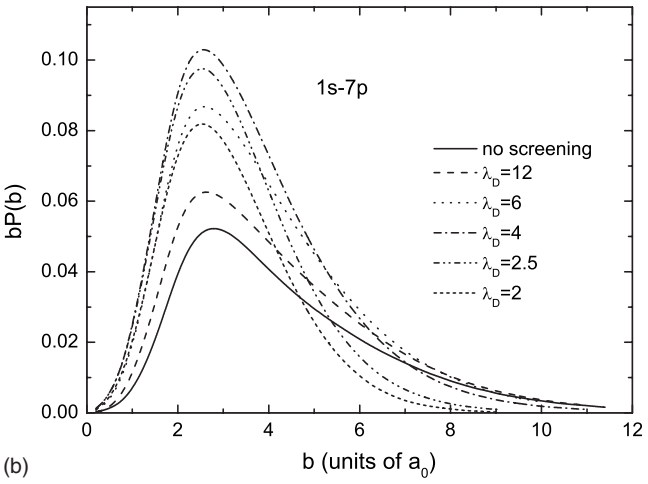


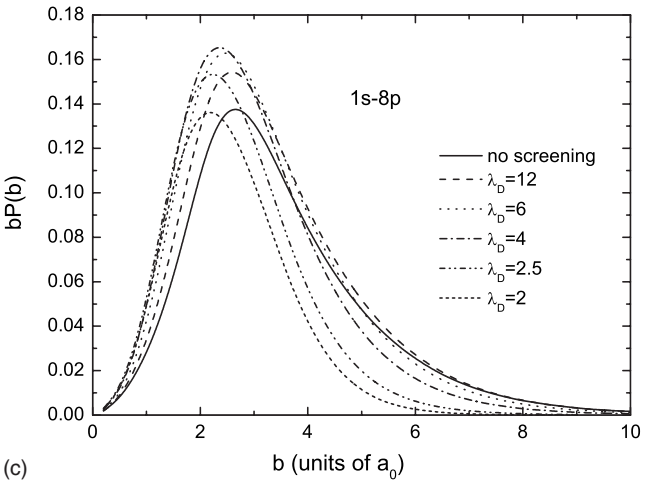


FIG. 6. Same as in Fig. 5, but for the collision energy of 100 keV/u.

=25 keV/u is their double peak structure. For the $7s$ and $7p$ pseudostates the peak at the small values of $b$ is not visible for $\lambda_D=2.5a_0$ and $\lambda_D=2a_0$, but for the $8p$ pseudostate it become noticeable even for these values of $\lambda_D$. We have identified that the peak at smaller $b$ values originates from transitions involving the $2s(He^+)$ and $2p(He^+)$ capture states.

The weighted probabilities $bP(b)$ for population of the same quasicontinuum states at E=100 keV/u [Figs. 6(a)–6(c)] do not exhibit a two peak structure such as those for 25 keV/u. This can be related to the much weaker

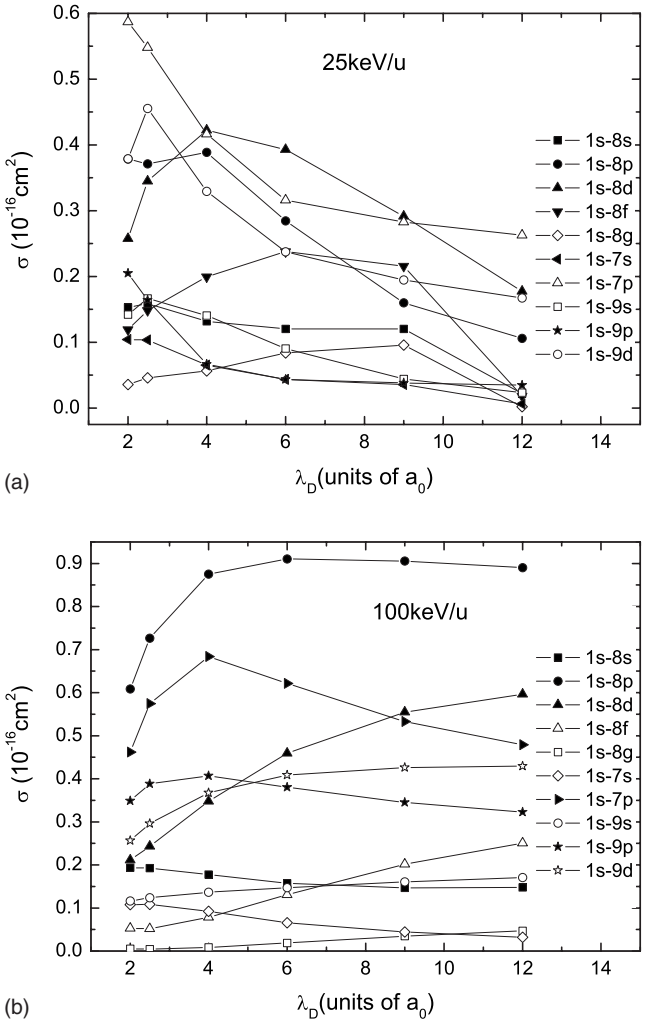


FIG. 7. $\lambda_D$-dependence of partial cross sections for the population of a number of target quasicontinuum states at collision energies of 25 keV/u (a) and 100 keV/u (b).

$1s(H)-2s$, $2p(He^+)$ exchange couplings at E=100 keV/u than for E=25 keV/u and to the shorter interaction time at the higher collision velocities. The probability $bP(b)$ for the $7s$ state increases with decreasing of $\lambda_D$, as in the case for E=25 keV/u, but for the states $7p$ and $8p$ it increases down $\lambda_D=4a_0$ and then starts to decrease. This $\lambda_D$ behavior of $bP(b)$ is strongly correlated with the $\lambda_D$ behavior of direct coupling matrix elements [Figs. 2(a)–2(c)] that are the dominant transition mechanisms at high energies.

### B. Ionization cross sections

It is of interest to investigate first the dependence of the partial ionization cross section for population of a given quasicontinuum state on the Debye length $\lambda_D$. Figures 7(a) and 7(b) show this dependence for a number of target quasicontinuum states at collision energies of 25 keV/u [panel (a)] and 100 keV/u [panel (b)]. The dominantly populated pseudostates at E=25 keV/u are $7p$, $8p$, $8d$, and $9d$, with the cross section for population of the $7p$ state continuously increasing with decreasing $\lambda_D$ down to $\lambda_D=2a_0$, while the population cross sections for $8p$ and $8d$ start to decrease for $\lambda_D$ below $\lambda_D=4a_0$ (and that for $9d$ below $\lambda_D=2.5a_0$). The cross sections for less populated pseudostates show similar nonmonotonic behavior with varying $\lambda_D$ at this collision energy. For E=100 keV/u [panel (b)], the population of the $8p$ state by far dominates in the entire range of $\lambda_D$ investigated and after the slow increase with decreasing $\lambda_D$ down to $\lambda_D=6a_0$ it starts to decrease. The cross section for significantly populated pseudostate $7p$ increases with decreasing $\lambda_D$ down to $\lambda_D=4a_0$ and then starts to decrease, while that for the $8d$ pseudostate decreases with decreasing $\lambda_D$ starting already with $\lambda_D=12a_0$. In view of the large number of different couplings populating these quasicontinuum states, all having a rather complex dependence on $\lambda_D$ (which for the exchange couplings depends also on the energy), it is difficult to make a transparent physical interpretation of the $\lambda_D$ behavior of pseudostate population cross sections. A mere observation that can be made from Figs. 7(a) and 7(b) is that, within a given $n$, the states with $l=1,2$ are dominantly populated ones.

As discussed in Sec. II B, the total ionization cross section contains contributions from the population of target-centered quasicontinuum states, $\sigma_{ion}^{tc}$, Eq. (11a), and population of the projectile-centered quasicontinuum states, $\sigma_{ion}^{pc}$, Eq. (11b). A projectile quasicontinuum state, $nl(He^+)$, can be populated only for $\lambda_D \leq \lambda_{D,c}^{n,l}$, when the corresponding discrete $nl(He^+)$ level from the projectile-centered basis $n \leq 4$ enters the continuum. This can be achieved by transitions from the discrete states (centered either on the target or projectile) when the level is already in the continuum, or by carrying out its population from the region $\lambda_D > \lambda_{D,c}^{n,l}$ (when it is a discrete state) into the region $\lambda_D \leq \lambda_{D,c}^{n,l}$ (when it becomes a continuum state). As also mentioned in Sec. II B, with our $n \leq 4$ basis centered on $He^+$, the ionization to the projectile continuum can take place only for $\lambda_D \leq 10.12a_0$, i.e., for screening length below the critical Debye length for the $4f(He^+)$ state (see Table II).

In Figs. 8(a) and 8(b) we show the energy dependence of the cross sections for ionization to target continuum (ITC) states, $\sigma_{ion}^{tc}$ [panel (a)], and ionization to projectile continuum (IPC) states, $\sigma_{ion}^{pc}$ [panel (b)], for the unscreened case (for $\sigma_{ion}^{tc}$ only) and for the interaction screening with $\lambda_D=12$, 6, 4, 2.5, and $2a_0$ in the energy range 5–300 keV/u. With decreasing $\lambda_D$, the ITC cross section first increases (with respect to the unscreened case) in the entire energy range considered down to $\lambda_D \leq 4a_0$, but then starts to decrease in the energy region above ~40 keV/u. This $\lambda_D$ behavior of ITC cross sections can be correlated with the similar behavior of direct coupling matrix elements in Fig. 2. The large values of ITC cross sections for $\lambda_D=2.5a_0$ and $\lambda_D=2a_0$ in the region below ~30 keV/u may be associated with the contribution to ITC by transitions from $2s(He^+)$ and $2p(He^+)$ quasiresonant capture states lying close to or in the continuum ($\lambda_{D,c}^{2s}=1.68a_0$, and $\lambda_{D,c}^{2s}=2.27a_0$, see Table II) and thereby strongly coupled with the low-lying target quasicontinuum states [such as $7p$, $8p$, $8d$; see Figs. 1(b) and 7(a)].

The IPC cross sections for $\lambda_D=6$, 4, 2.5, and $2a_0$ [Fig. 8(b)] have significant values only for energies below ~60 keV/u, increasing sharply with decreasing $\lambda_D$. For $\lambda_D=6a_0$, only the $4l$ $(He^+)$ states are in the continuum (see Table II), and the IPC cross section is relatively small. For

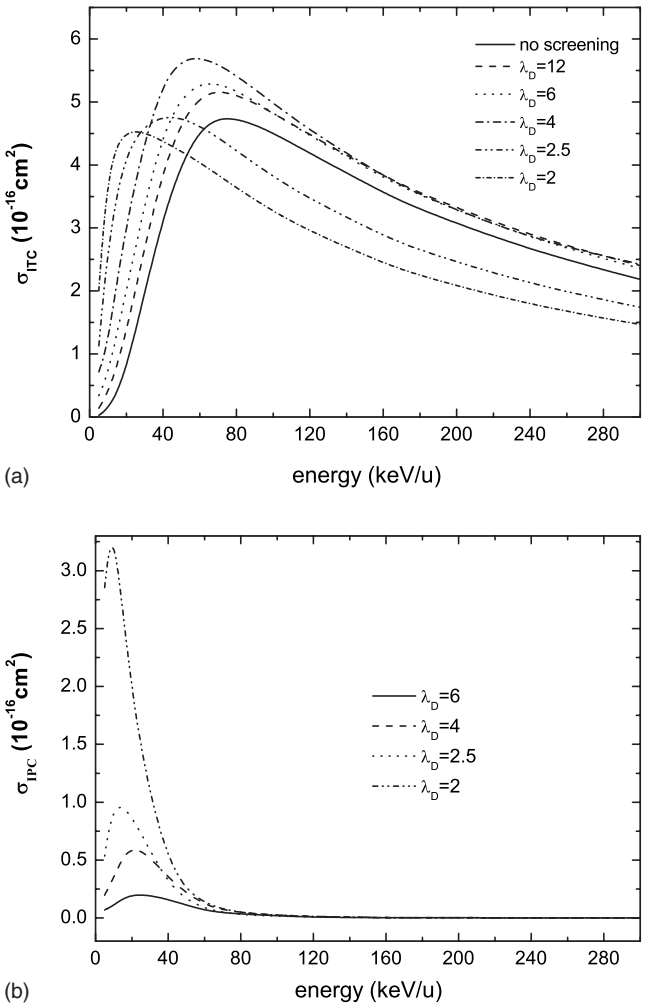


FIG. 8. Energy dependence of cross sections for ionization to target continuum (ITC) states (a) and ionization to projectile continuum (IPC) states (b) for the unscreened case (for $\sigma_{ion}^{tc}$ only) and for the interaction screening with $\lambda_D=12$, 6, 4, 2.5, and $2a_0$.

$\lambda_D=4a_0$, the $3p$, $3d$, and $4l$ $He^+$-centered states are in the continuum, while for $\lambda_D=2.5a_0$ the $3s(He^+)$ state also becomes a quasicontinuum state, contributing to the further increase of the IPC cross section. For $\lambda_D=2a_0$, the $2p(He^+)$ state, quasiresonantly coupled with the initial $1s$(H) state, becomes also a quasicontinuum state, leading to a drastic increase of the IPC cross section with respect to the $\lambda_D=2.5a_0$ case.

The energy dependence of total ionization cross section, $\sigma_{ion}=\sigma_{ion}^{tc}+\sigma_{ion}^{pc}$, is shown in Fig. 9 for the unscreened case and for interaction screening with $\lambda_D=12$, 6, 4, 2.5, and $2a_0$. Obviously, it differs from the ITC cross section shown in Fig. 8(a) only in the energy region below ~60 keV/u where the contribution of $\sigma_{ion}^{pc}$ is considerable. In this figure the theoretical ionization cross sections of Refs. [17,18] and the experimental cross section of Ref. [23] are also shown. Our cross section for the zero-screening case practically coincides with that of Ref. [18] in the overlapping energy range (above 20 keV/u) and with the experimental data. The slight oscillatory behavior of the cross section of Ref. [17] around that of Ref. [18] (and ours) is most probably an artifact of the

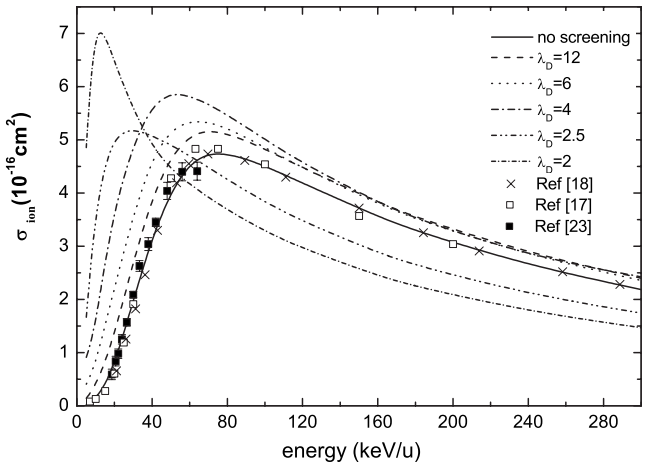


FIG. 9. Total ionization cross section, $\sigma_{ion}=\sigma_{ion}^{tc}+\sigma_{ion}^{pc}$, for the unscreened case (solid line) and for interaction screening with $\lambda_D=12$, 6, 4, 2.5, and $2a_0$ (other lines) as a function of collision energy. The crosses and open squares are the results of TCAOCC calculations of Refs. [18,17], respectively, and the closed squares are the experimental data of Ref. [23].

quasisymmetric two-center basis used in Ref. [17] (all $n\leq 4$ discrete and 84 quasicontinuum states on H and all $n\leq 5$ discrete and 61 quasicontinuum states on $He^+$), as demonstrated in Ref. [18]. We remind that the basis set used in the present calculations differs from that in Ref. [18] in the number of projectile-centered states only (in our case are all $n\leq 4$ discrete states, while in Ref. [18] all $n\leq 5$ states) while the number of target-centered states is the same (all $n\leq 6$ and $7s$ discrete states and 117 quasicontinuum states). The coincidence of our total ionization cross section with that of Ref. [18] confirms the arguments given in Refs. [18,21] regarding the limited required size of the projectile centered basis for description of the ionization process, provided that the target-centered basis is large enough and contains a large number of continuum states, and thus justifies the adequacy of the basis adopted in the present study.

## IV. CONCLUSIONS

In the present work we have studied the dynamics of the ionization process in the $He^{2+}+H(1s)$ collision system with screened Coulomb interactions of type (2) by using the TCAOCC method. A large basis of atomic orbitals was employed on both centers, including 117 target-centered quasicontinuum states even in the limit of zero screening. The main effect of the screened Coulomb interactions in the system on the ionization dynamics is the reduction of the number of bound states and the simultaneous increase of the number of quasicontinuum states (centered both on the target and the projectile) when the interaction screening increases. The change of wave functions and energies of both discrete and quasicontinuum states with varying the screening parameter introduces changes in the couplings between these states, thus affecting the ionization dynamics as well.

With decreasing the screening length, the cross section for ionization to target continuum (ITC) states in the energy re-

gion above ~50 keV/u first increases with respect to the zero-screening case (due to the increase of the number of quasicontinuum states), but for screening lengths below $\sim 3a_0$ it starts to decrease (due to drastic reduction of the number of intermediary discrete states and of the direct coupling matrix elements). In the energy region below ~50 keV/u, the ITC cross section again increases (with respect to the zero-screening case) with decreasing $\lambda_D$ due to transitions via the $n=2$ $He^+$ capture states, strongly (resonantly) coupled with the initial $1s$(H) state at these energies. The ionization to the projectile-centered continuum states (IPC) becomes important only at collision energies below ~60 keV/u and for screening lengths below $\sim 6a_0$. The IPC cross section sharply increases with decreasing $\lambda_D$ and gives a significant contribution to the total ionization cross section at collision energies below ~30 keV/u. The observed strong increase of total ionization cross section (with respect to the zero screening case) with decreasing $\lambda_D$, especially for collision energies below ~50 keV/u, obviously has important effects on the collision kinetics and properties of a Debye plasma, drastically increasing, for instance, its stopping power.

Although the present study of the ionization dynamics of a collision system with Debye screening of Coulomb interactions was performed for the specific case of a $He^{2+}+H(1s)$ system, its main conclusions should obviously remain valid for any one-electron collision system, and even for collision systems with more than one electron. Indeed, reduction of the number of discrete states (and the simultaneous increase of continuum states) with decreasing the screening length, which is one of the main elements affecting the ionization dynamics, is a general quantum-mechanical property of short-range potentials [20], that for a number of two-electron atomic systems has been demonstrated in Ref. [24].

## ACKNOWLEDGMENTS

One of us (R.K.J) would like to acknowledge the warm hospitality of the Institute of Applied Physics and Computational Mathematics during the period when this work was performed. We thank C. D. Lin for use of his AOCC code. This work was partly supported by the National Natural Science Foundation of China (Grants No. 10574018, No. 10574020, No. 10734140, and No. 10604011).

[1] J. C. Weisheit, in *Applied Atomic Collision Physics*, edited by C. F. Barnett and M. F. A. Harrison (Academic, New York, 1984), Vol. 2.
[2] J. C. Weisheit, Adv. At. Mol. Phys. **25**, 101 (1988).
[3] M. S. Murillo and J. C. Weisheit, in *Strongly Coupled Plasma-Physics*, edited by H. M. Van Horn (University of Rochester Press, Rochester, NY, 1993), p. 233.
[4] M. S. Murillo, in *Atomic Processes in Plasmas*, edited by A. L. Osterheld and W. H. Goldstein, AIP Conf. Proc. No. 381 (American Institute of Physics, Woodbury, NY, 1996), p. 231.
[5] E. L. Pollock and J. C. Weisheit, in *Spectral Line Shapes*, edited by F. Rostas (Walter de Gruyter, New York, 1985), Vol. 3, p. 181.
[6] B. L. Whitten, N. F. Lane, and J. C. Weisheit, Phys. Rev. A **29**, 945 (1984); **30**, 650 (1984).
[7] J. K. Yuan, Y. S. Sun, and S. T. Zheng, J. Phys. B **29**, 153 (1996).
[8] Y.-D. Jung, Phys. Plasmas **2**, 332 (1995); **2**, 1775 (1995).
[9] Y.-D. Jung, Phys. Plasmas **4**, 21 (1997).
[10] Y.-D. Jung and J.-S. Yoon, J. Phys. B **29**, 3549 (1996).
[11] K. Scheibner, J. C. Weisheit, and N. F. Lane, Phys. Rev. A **35**, 1252 (1987).
[12] C.-G. Kim and Y. -D. Jung, Phys. Plasmas **5**, 2806 (1998); **5**, 3493 (1998).
[13] Y.-D. Jung, Europhys. Lett. **69**, 753 (2005).
[14] H. Zhang, J. G. Wang, B. He, Y. B. Qiu, and R. K. Janev, Phys. Plasmas **14**, 053505 (2007).
[15] W. Fritsch and C. D. Lin, Phys. Rep. **202**, 1 (1991).
[16] L. Liu, J. G. Wang, and R. K. Janev, Phys. Rev. A **77**, 032709 (2008).
[17] N. Toshima, Phys. Rev. A **50**, 3940 (1994).
[18] J. Kuang and C. D. Lin, J. Phys. B **30**, 101 (1997).
[19] C. M. Reeves, J. Chem. Phys. **39**, 1 (1963).
[20] L. D. Landau and E. M. Lifshitz, *Quantum Mechanics: Non-Relativistic Theory* (Pergamon, London, 1958).
[21] J. Kuang and C. D. Lin, J. Phys. B **29**, 1207 (1996).
[22] F. J. Rogers, H. C. Graboske, and D. J. Harwood, Phys. Rev. A **1**, 1577 (1970).
[23] M. B. Shah and H. B. Gilbody, J. Phys. B **14**, 2361 (1981).
[24] T. Hashino, S. Nakazaki, T. Kato, and H. Kashiwabara, Phys. Lett. A **123**, 236 (1987).